

Synthesis of Polycrystalline Diamond Films in Abnormal Glow Discharge and their Properties

A V Gaydaychuk, S A Linnik, A V Kabyshev, F V Konusov and G E Remnev

National Research Tomsk Polytechnic University, 30, Lenin Avenue, 634050, Tomsk, Russia

E-mail: konusov@hvd.tpu.ru, stepan_lin@mail.ru

Abstract. The optical and electrophysical properties of polycrystalline diamond films (PDF) deposited from the abnormal glow discharge have been studied. The dominating mechanisms of absorption and charge carrier transfer and the energy spectrum of the localized states (LS) of defects which determine the properties of the films have been specified. The parameters of the interband absorption and electrical conductivity are determined by the continuous energy distribution in the band gap (BG) of the states of defects of different nature. The absorption edge of the crystalline phase of the films is separated from the absorption zone determined by the electron transitions between LS defects. The width of BG is narrowed to 0.2–0.5 eV from the quantity typical to the diamond. An additional film absorption edge is formed in the energy interval 1.2–3.3 eV, where Urbach rule is fulfilled and the interband absorption is realized at direct transitions through the optical gap 1.1–1.5 eV. The average width of BG is 2.6–3.24 eV estimated within semiclassical interband model. The interaction of the parameters of the interband and exponential absorption is determined by the crystal lattice static disorder. The dominating n-type of the activation component of the electrical conductivity is complemented by the hopping mechanism with the participation of the localized states of the defects distributed near the Fermi level with a density $5.6 \cdot 10^{17} - 2.1 \cdot 10^{21} \text{ eV}^{-1} \cdot \text{cm}^{-3}$.

Keywords: polycrystalline diamond films, absorption, electrical conductivity, photoconductivity, localized states of defects

1. Introduction

The unique chemical, mechanical, electrical and thermophysical, optical and photoelectrical properties of a diamond contribute to its wide application in high-frequency and high-temperature electronics [1–5]. Due to the limited potentials for application of diamond single crystals and epitaxial diamond films caused by their high cost, the most appropriate instruments are the polycrystalline diamond films (PDF), which are obtained by well-studied methods of the gas-phase deposition [1–9]. PDF are successfully used for the production of the stable radiation-resistant UV detectors and ionizing radiation, as well as for laser and photodiode structures [1,4–7]. Depending on the characteristics of PDF polycrystalline structure, the content of alloying impurity atoms and defects in the PDF crystal structure, their optical and electrical characteristics vary widely. It stimulates the study of the electrophysical and optical properties of PDF, the investigation of the mechanisms determining these properties and the influence of deposition conditions on the change in the characteristics. The method



of the film deposition from abnormal glow discharge (AGD) plasma stands out among various methods of PDF deposition – using microwave discharge plasma, hot filament, and plasma-arc CVD. Each of the methods has a lot of disadvantages: high cost and/or limitations in maximum deposition area; low rate and the necessity to repeated replacement of filaments; the drawback of a plasma-arc CVD method is a small deposition area and high gas consumption. The efficiency of the method of PDF deposition from AGD plasma compared to the alternative ones is in its simplicity and a high growth rate.

The aim of the work is to determine the optical, electrical, and photoelectrical characteristics, the energy spectrum of the defect levels and their nature in PDF deposited from AGD plasma.

2. Research methods

The methods of film deposition from AGD and the study of the film structural features are described in detail in [2, 3]. A new system of diamond film deposition from AC of AGD has been presented. In the process of deposition the discharge in the form of the plasma filament is realized between two small electrodes, and the distance between electrodes reaches 20 cm. The electrodes are removed from the substrate, and the material of the electrodes does not contaminate the film [2]. The absorption spectra of $\alpha(h\nu)$ were calculated from the diffuse reflection spectra and were approximated by the Urbach rule to determine the characteristics of the localized states (LS) of defects distributed in the band gap (BG) of the films and by the laws for the interband absorption of crystalline and amorphous semiconductors [10]. The dark surface conductivity σ and photoconductivity $\Delta\sigma_{ph}=\sigma_{ph}-\sigma$ (σ_{ph} is conductivity under lighting), photosensitive $K(U, T, h\nu)=\Delta\sigma_{ph}/\sigma$ were measured at a constant voltage across the electrodes $U=0.01-300$ V, at temperature $T=300-700$ K and photon energy $h\nu=1.5-4.0$ eV. The electrodes were deposited on the surface by rubbing the soft graphite. The temperature dependences of σ and $\Delta\sigma_{ph}(T)$ were approximated by the equation for the activation mechanism

$$\sigma_a(T) = \sigma_0 \times e^{(-\varepsilon_\sigma/k-T)} \quad (1)$$

(σ_0 is a pre-exponential factor, ε_σ is an activation energy, k is the Boltzmann constant) and by the equation for the hopping mechanism of transfer between LS near the Fermi level E_F within the Mott model

$$\sigma_p(T) = \sigma'_0 \times e^{-(T_0/T)^{0.25}}, \quad (2)$$

(σ'_0 is a pre-exponential factor, T_0 is activation energy) [11, 12]. The LS density $N(E_F)$ near E_F was calculated from T_0 according to [11, 12]. The sign of the dominant charge carriers was determined by the photostimulated current amplitude $I_{phTSC}(T, h\nu, U=0)$ [11].

3. Results and discussion

The $\alpha(h\nu)$ spectra indicate the heterogeneity of defect pattern with LS when $h\nu=1.1-5.5$ eV (figure 1). The concentration of LS defects vary from $N=2 \cdot 10^{19}$ to $3 \cdot 10^{20}$ cm⁻³ across the surface of the film deposition and over their thickness (figure 1). The surface roughness has a greater effect on the properties than the size of the crystallites [1]. The accumulation of LS with an energy of $h\nu=1.1-1.9$ and $2.5-4.5$ eV is higher from the side of the substrate than from the growth side (figure 1). The characteristics of $\alpha(h\nu)$ spectra indicate the dominant defect agglomeration near the intercrystalline boundaries of PDF and the impact of the amorphous hydrogenated carbon a-C:H by analogy with [1, 6-9]. A sharp rise of α when $h\nu>5.0$ eV responds the fundamental absorption in crystallites (figure 1). The width of BG films $E_g=5.0-5.27$ eV for direct transitions when $h\nu=5.2-5.6$ eV is close to $E_g=5.45$ eV of diamond and $E_g=5.0-5.5$ eV of CVD films [1, 4-5]. The absorption in PDF crystallites ($h\nu=5.0-5.6$ eV) is separated from the absorption zone ($h\nu=1.1-5.0$ eV) caused by defect LS (figure 1). BG narrowing by $0.1-0.2$ eV is more explicitly from the side of the substrate to the edge of deposition. The spectra indicate the realization within the interval $h\nu=1.1-5.0$ eV of several types of absorption. Within the intervals $h\nu=1.18-1.3$, $1.3-1.8$, and $1.8-2.3$ eV the spectra $\alpha(h\nu)$ obey the Urbach rule

$$\alpha(h\nu) = \alpha_0 \times e^{(-h\nu/E_U)} \quad (3)$$

with the PDF typical parameters α_0 and E_U (E_U is Urbach energy) (figure 1). In the intervals $h\nu=1.18-1.3$ eV the value $E_U=0.05-0.2$ eV is close to the value E_U in a-C:H [8]. The big values $E_U>1.6$ eV within the intervals $h\nu=1.3-1.8$, $1.8-2.3$ eV in the films are typical to nanocrystalline diamond films (NCDF) [1, 5, 6, 9, 13, 14]. Increasing E_U with the depth of the level in BG is determined by the high overlapping of exponentially distributed LS and enables the realization of interband absorption at the distance from the edge of BG. The characteristics of exponentially distributed levels in BG are determined by a high impact of graphite-like phase disordered by the defects [1, 6-9].

The spectra $\alpha(h\nu)$ are also approximated by the law for the interband absorption

$$\alpha \times h\nu = B'(B'') \times (h\nu - E'_g(E''_g))^m, \quad (4)$$

where $m=1/2$ and 2 for direct and indirect allowed transitions through the optical bands E'_g and E''_g , respectively. For the indirect transitions realized within the interval $h\nu=1.2-2.4$ eV, $E''_g \leq 0$ eV, and for the direct within the interval $h\nu=1.5-3.4$ eV the BG width is $E'_g=1.1-1.6$ eV (figure 2). It indicates the probable overlapping of LS with the allowed bands caused by the increase in the content of sp^2 clusters and their sizes by analogy with [1]. In NCDF the close interrelations ($E''_g=1.0$ eV, $E'_g=2.2$ eV) are determined by the defect LS near the grain boundaries [15, 16]. In the films a-C and a-C:H $E''_g=1-3$ and $1.5-3.5$ eV [8]. In PDF E''_g is narrower than in the diamond-like carbon films (DLCF) and ultradispersed nanodiamond films (UDNDF), where $E''_g=3.3-3.5$ eV. The interval overlap of the interband and exponential absorption suggests that a new edge of absorption is formed in PDF biased to the zone $h\nu=1.2-3.3$ eV, where the Urbach rule is followed and the interband absorption is realized. The decrease in E_g with E_U growing is typical to LS with $h\nu=1.18-1.3$ and $1.8-2.3$ eV (figure 3). The similar interrelation E''_g and E_U is typical to the films a-C, a-C:H [8] and to the materials with a high concentration of defects [10].

The effect of the structural disorder in PDF is estimated and within the semiclassical model for the interband absorption of amorphous or highly defect materials [1, 10]. Here the spectra obey the law

$$\alpha(h\nu) = \alpha''_0 \times e^{-(h\nu - E_{g0})^2 / 2\sigma^2}, \quad (5)$$

where α''_0 is a multiplier, E_{g0} is a mean BG width (E_g obeys the Gaussian distribution relative to E_{g0} , σ^2 is the dispersion of the value E_g determined by the disorder induced by defects) (figure 1, curve 2). The dispersion σ is close to the value E_U for the defects localized when $h\nu=1.3-1.8$ eV. The values E'_g and E_{g0} correlate due to the equality of both interband absorption models (figure 3). Since the overlapping degree of the defect levels is growing ($\sim E_U$), the mean BG width E_{g0} is decreased (figure 3). The values α''_0 and B' (proportional to the density of states bound by the interband transitions through the optical gap) vary in the correlation when E_{g0} is changed (figure 4). The values E_{g0} in PDF are close to the optical gap of DLCF $E''_g=3.77$ eV and UDNDF $E_g=3.3-3.5$ eV. The PDF spectra $\alpha(h\nu)$ correspond to the transition model between the states $\pi-\pi^*$ determined by the border inclusions a-C, through the pseudogap $E_{g0}=3.0-3.5$ eV [1, 6, 7, 9, 17]. The correlations between the parameters E_g , E_{g0} and σ , E_U are typical to the materials with the static and/or dynamic disorder of the crystal lattice (figures 3 and 4) [10, 14-16]. It indicates the impact of the absorption in crystallites on the properties, and it suggests that PDF is the material with the BG width for direct transitions $1.1-1.6$ eV and the absorption edge determined by the defect LS with $\varepsilon=1.2-3.3$ eV.

Spectrum factorization on the elementary Gaussian curves $\alpha \sim \exp(-(h\nu - E)^2 / (0.833 \cdot \gamma^2))$ (E is the center, γ is half-width) identify the local defect levels: **1**- $E=1.17$ eV, $\gamma=0.1$ eV, $N=2 \cdot 10^{19}$ cm^{-3} (V^+ is the center [14]); **2**- 1.4 eV, 0.3 eV, $1.2 \cdot 10^{20}$ cm^{-3} ; **3**- $(1.8-2)$ eV, 0.4 eV, $7 \cdot 10^{20}$ cm^{-3} (GR1, I^0 are the centers [18]); **4**- $(2.1-2.2)$ eV, 0.2 eV, $2 \cdot 10^{19}$ cm^{-3} ($sp^2(\pi \rightarrow \pi^*)$ [1, 7]); **5**- $(2.6-2.7)$ eV, 0.5 eV, $2 \cdot 10^{20}$ cm^{-3} ($sp^2(\pi \rightarrow \pi^*)$ [1, 7]); **6**- $(3.2-3.4)$ eV, 0.4 eV, $3 \cdot 10^{20}$ cm^{-3} (V^- , $sp^2(\pi \rightarrow \pi^*)$ [1, 6]); **7**- $(3.9-4.1)$ eV, 0.4 eV, $2 \cdot 10^{20}$ cm^{-3} (N4-6, $sp^2(\pi \rightarrow \pi^*)$ [1, 7]); **8**- $(4.4-4.6)$ eV, 0.3 eV, $7 \cdot 10^{19}$ cm^{-3} (Σ - Σ^*) [1, 6, 7]). The defects are distributed both in crystallites and at the intercrystalline PDF boundaries.

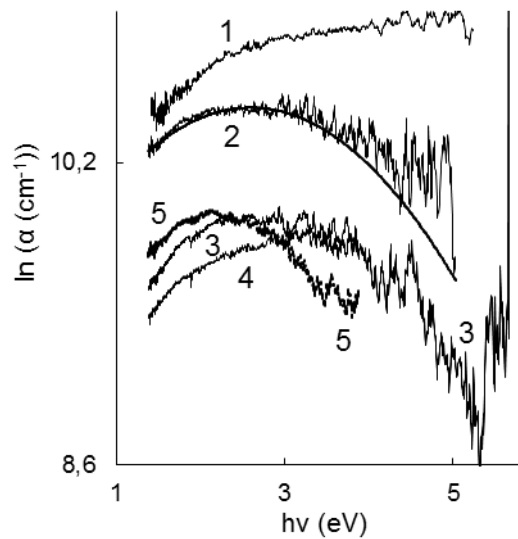


Figure 1. The absorption spectra $\alpha(h\nu)$ of PDF with the side of the substrate (1–3) and growth (4, 5) at the edge (1, 2, 5) and in the deposition center (3, 4) and their approximation (2) with the equation (5) at $E_{g0}=2.6$ eV and $\sigma=1.8$ eV.

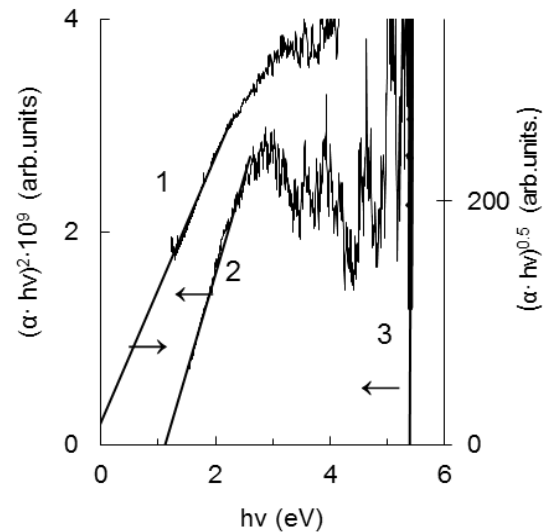


Figure 2. The spectra of interband PDF absorption with indirect (1) and direct allowed transitions (2, 3) through the optical gaps E''_g and E'_g , respectively.

The photosensitivity spectra $K(h\nu)$ are similar to the film absorption spectra and typical to the diamond films [1, 4, 9, 11]. The spectra $K(h\nu)$ are determined by the electron transitions between the valence band and defect LS. Some definite contribution to $K(h\nu)$ is made by the transitions between the “tails” of the LS of the allowed bands and the levels associated with the graphite-like phases [1, 11]. The oxygen molecules adsorbed on the film surface facilitate the increase in UV photosensitivity due to their passivating action on defect LS [11].

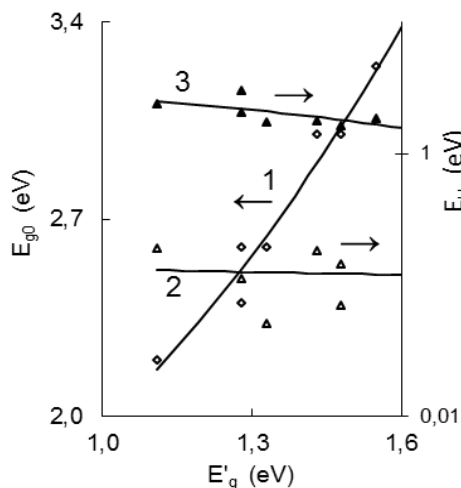


Figure 3. $E_{g0}(E'_g)$ (1) vs. $E_U(E'_g)$ (2, 3) in PDF. The value E_{g0} is calculated within the interval $h\nu=1.2-5$ eV, E'_g within the interval $h\nu=1.5-3.4$ eV, and E_U within the interval $h\nu=1.18-1.3$ (2) and $1.8-2.3$ eV (3)

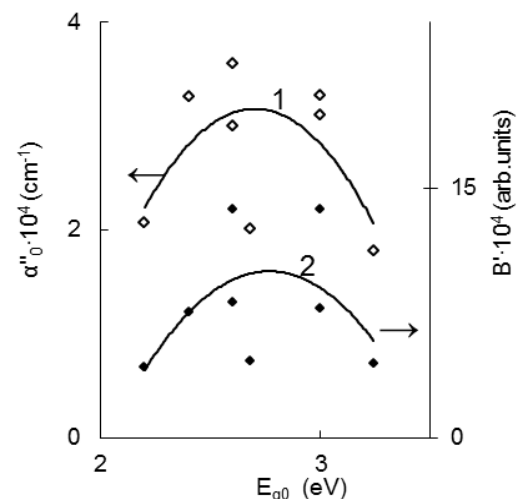


Figure 4. $\alpha''_0(E_{g0})$ (1) vs. $B'(E_{g0})$ (2) in PDF. The value E_{g0} is calculated within the interval $h\nu=1.2-5$ eV, and the value B' within the interval $h\nu=1.5-3.4$ eV.

Volt-ampere characteristics, field dependence of photosensitivity $K(U)$, energy and kinetic characteristics of electrotransfer $\epsilon_\sigma, \sigma_0, T_0, \sigma'_0, N(E_F), I_{phTSC}$ vary in the thickness and in the PDF deposition plane caused by the heterogeneity of their properties [11]. The temperature dependencies of $\sigma, \Delta\sigma_{ph}(T)$ within the interval $T=300-600$ K are determined by the thermally stimulated electron exchange between the shallow donor levels with an energy $\epsilon_\sigma=0.007-0.21$ eV and the conduction band (CB) [11]. The dominating n-type of σ and $\Delta\sigma_{ph}$, as the dependencies $I_{phTSC}(T, hv)$ show [11]. We cannot exclude the effect of the holes exchange between defect LS and the valence band on the characteristics of the films. The electrical parameters indicate the effect on the transport of the hopping conductivity that is verified by the approximation $\sigma(K)$ by the equation (2) within the interval $\Delta T=300-600$ K [11]. The LS density calculated from the dependencies $\sigma, \Delta\sigma_{ph}(T)$ is $N(E_F)=5.6 \cdot 10^{17}-1.5 \cdot 10^{21} \text{ eV}^{-1} \cdot \text{cm}^{-3}$ in PDF with $\epsilon_\sigma=0.007-0.15$ eV. In PDF deposited by the alternative methods, the density of LS exponentially distributed near E_F is $N(E_F)=(4-8) \cdot 10^{19}$ [7, 12] and $10^{15}-10^{18} \text{ eV}^{-1} \cdot \text{cm}^{-3}$ [19]. The value of the most probable length of the hop calculated using the values $N(E_F)$ is $R=1.1-8.1$ nm and is decreased at lightning to 1.0–6.0 nm under the increase in the density of the states by 3–5 times for the films with electrical conductivity $\sigma < 10^{-10}$ S [11].

The correlations between σ_p, σ_a and K enable to make the dominance of one of the transport mechanisms [11]. The dominance of σ_a is verified by the dependence $N(E_F)(\epsilon_\sigma)$, which is typical to the noncrystalline semiconductors, which have a high concentration of defects (figure 5) [7, 11, 12, 19]. In PDF, the hopping LS conductivity near E_F predominates over the activation one at $T=300-400$ K. When $T=400-600$ K, the PDF characteristics are determined by $\sigma_a(T)$ involving LS defects distributed at the grain boundaries and localized in the BG in the region of the “tails” of the allowed bands [11]. When $T > 600$ K, the effect of the energy barrier between crystallites on the transport is increased [11]. The established interrelation between the characteristics α, ϵ_σ , and E'_g agree with the models of the electrotransfer typical for amorphous and highly defect materials [10, 11]. The accumulation of the concentration of absorption centers is related with the decrease in the LS density which participate in the hopping of σ_p from $N(E_F)=10^{19}$ to $5 \cdot 10^{17} \text{ eV}^{-1} \cdot \text{cm}^{-3}$ in the correlation with the increase in α from $2 \cdot 10^4$ to $5 \cdot 10^4 \text{ cm}^{-1}$ (figures 1 and 5). The decrease in σ and $N(E_F)$ correlate with the increase in ϵ_σ and E_U for LS at $h\nu=1.15-1.3$ eV and $1.6-3.0$ eV (figures 5 and 6). The growth of E_U from 0.07 to 0.15 eV, as σ is decreased from $\sigma=10^{-4}$ to 10^{-11} S and ϵ_σ is increased from 0.007 to 0.16 eV, is determined

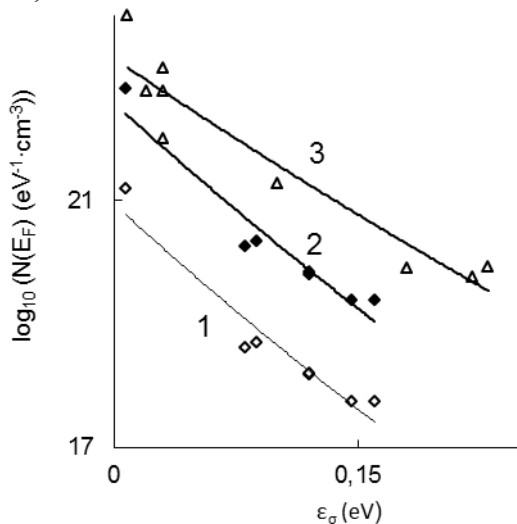


Figure 5. Interrelation between LS density and activation energy ϵ_σ in the deposited films (1, 2) and according to [7] (3). Attenuation constant $\alpha=5.7 \cdot 10^6$ (1) and $2 \cdot 10^7 \text{ cm}^{-1}$ (2).

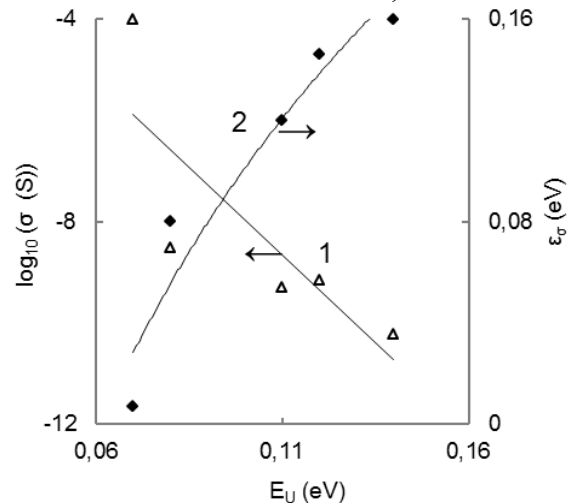


Figure 6. Interrelation between conductivity σ Urbach energy E_U (1) and activation energy ϵ_σ and E_U (2) in the deposited films. The values E_U are calculated within the interval $h\nu=1.15-1.3$ eV.

by the impact of the structural disorder induced by defects in the film material and the impact of the disordered graphite-like phases [10, 11]. In the film material BG, the LS energy exponential distribution is formed, LS are induced by the growth defects [1, 10, 11].

4. Conclusion

The properties of the films deposited from AGD do not yield to those of the diamond films obtained by the alternative methods. PDF absorption deposited from the AGD plasma is determined by the continuous LS spectrum induced by different imperfections. The edge of PDF absorption when 5.0–5.6 eV is separated from the absorption zone within the interval 1.1–5.0 eV induced by defect LS. The BG width is narrowed to $E_g=5.0-5.3$ eV. The absorption in the energy interval of 1.0–5.0 eV is realized with the transitions between defect LS and interband transitions which are typical to the crystalline and amorphous materials. A new edge of absorption is formed in the films in the energy interval of 1.2–3.3 eV, where the Urbach rule is followed the interband absorption is realized by the direct and indirect transitions. The electrical characteristics of the films are determined by the structural disorder induced by the growth defects in crystallites and by the presence of graphite-like phases in the films. The n-type conductivity activation component is realized when the electrons are exchanged between CB and donor levels with an energy ≤ 0.21 eV and is amplified by the LS hopping mechanism near the Fermi level with a density of $5.6 \cdot 10^{17} - 2.1 \cdot 10^{21}$ eV⁻¹·cm⁻³.

Acknowledgments

The paper has been completed within megaproject of National Research Tomsk Polytechnic University (VIU_IHTPh_85_2014) «Materials for Extreme Conditions».

References

- [1] Williams O A 2011 *Diamond and Relat. Mater.* **20** 621
- [2] Linnik S A and Gaydaychuk A V 2013 *Diamond and Relat. Mater.* **32** 43
- [3] Linnik S A and Gaydaychuk A V 2012 *Tech. Phys. Lett.* **38** 258
- [4] Ralchenko V, Pimenov S and Konov V 2007 *Diamond and Relat. Mater.* **16** 2067
- [5] Willems B, Tallaire A and Achard J 2014 *Diamond and Relat. Mater.* **41** 25
- [6] Varga M, Remes Z, Babchenko O and Kromka A. 2012 *Phys. Stat. Sol.* **B249** 2635
- [7] Achatz P, Garrido J A, Stutzmann M, Williams O A, Gruen D M, Kromka A and Steinmüller D 2006 *Appl. Phys. Lett.* **88** 101908
- [8] Fanchini G and Tagliaferro A 2004 *Diamond and Relat. Mater.* **13** 1402
- [9] Vanesek M, Rosa J, Nesladek M and Stals L M 1996 *Diamond and Relat. Mater.* **5** 952
- [10] Konusov F V, Kabyshev A V and Remnev G E 2011 *J. of Surface Invest.* **5** 228
- [11] Konusov F V, Kabyshev A V, Linnik S A, Gaydaychuk A V and Remnev G E 2014 *J. of Phys.: Conf. ser.* **552** 012046
- [12] Gan L, Bolker A, Saguy C, Kalish R, Tan D L, Tay B K, Gruen D and Bruno P 2009 *Diamond and Relat. Mater.* **18** 1118
- [13] Nebel C E, Reisel R and Stutzmann M 2001 *Diamond and Relat. Mater.* **10** 639
- [14] Sharda T, Rahaman M M, Nukaya Y, Soga T, Jimbo T and Umeno M 2001 *Diamond and Relat. Mater.* **10** 361
- [15] Nagano Akira, Yoshitake Tsuyoshi, Hara Takeshi and Nagayama Kunihiro 2008 *Diamond and Relat. Mater.* **17** 1199
- [16] Franta D, Zajičková L, Karásková M, Jašek O, Nečas D, Klapetek P and Valtr M 2008 *Diamond and Relat. Mater.* **17** 1278
- [17] Mathioudakis C, Kopidakis G, Patsalas P and Kelires P C 2007 *Diamond and Relat. Mater.* **16** 1788
- [18] Jones R 2009 *Diamond and Relat. Mater.* **18** 820
- [19] Nath S and Wilson J I B 1996 *Diamond and Relat. Mater.* **5** 65